AD-A110 622 MEGAPULSE INC BEDFORD MASS F/G 17/9
INSTRUMENTATION FOR THE MEASUREMENT OF THE SPECTRAL DENSITY OF --ETC(U)
DEC 81 R C KAHLER, J B DONOHOE F19628-80-C-0092
UNCLASSIFIED RADC-TR-81-346 NL

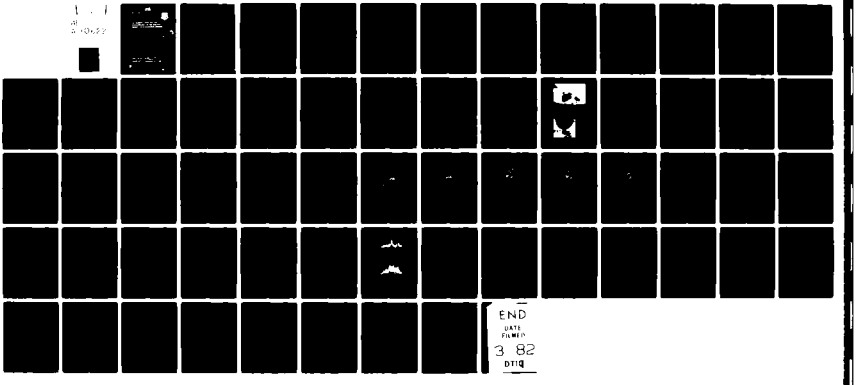

END
DATE FILMED
3 82
DTIC

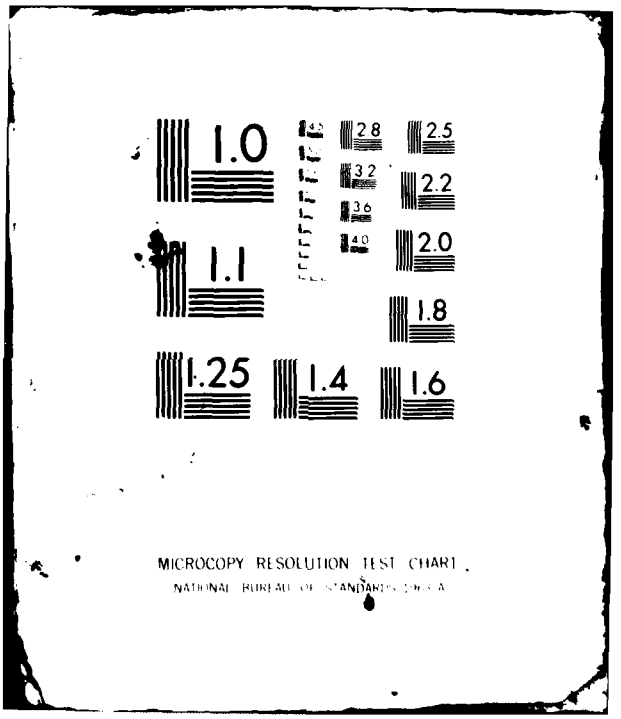
1.0
1.1
1.25
1.4
1.6
1.8
2.0
2.2
2.5
2.8
3.2
3.6
4.0
MICROCOPY RESOLUTION TEST CHART
NATIONAL BUREAU OF STANDARDS-1963-A

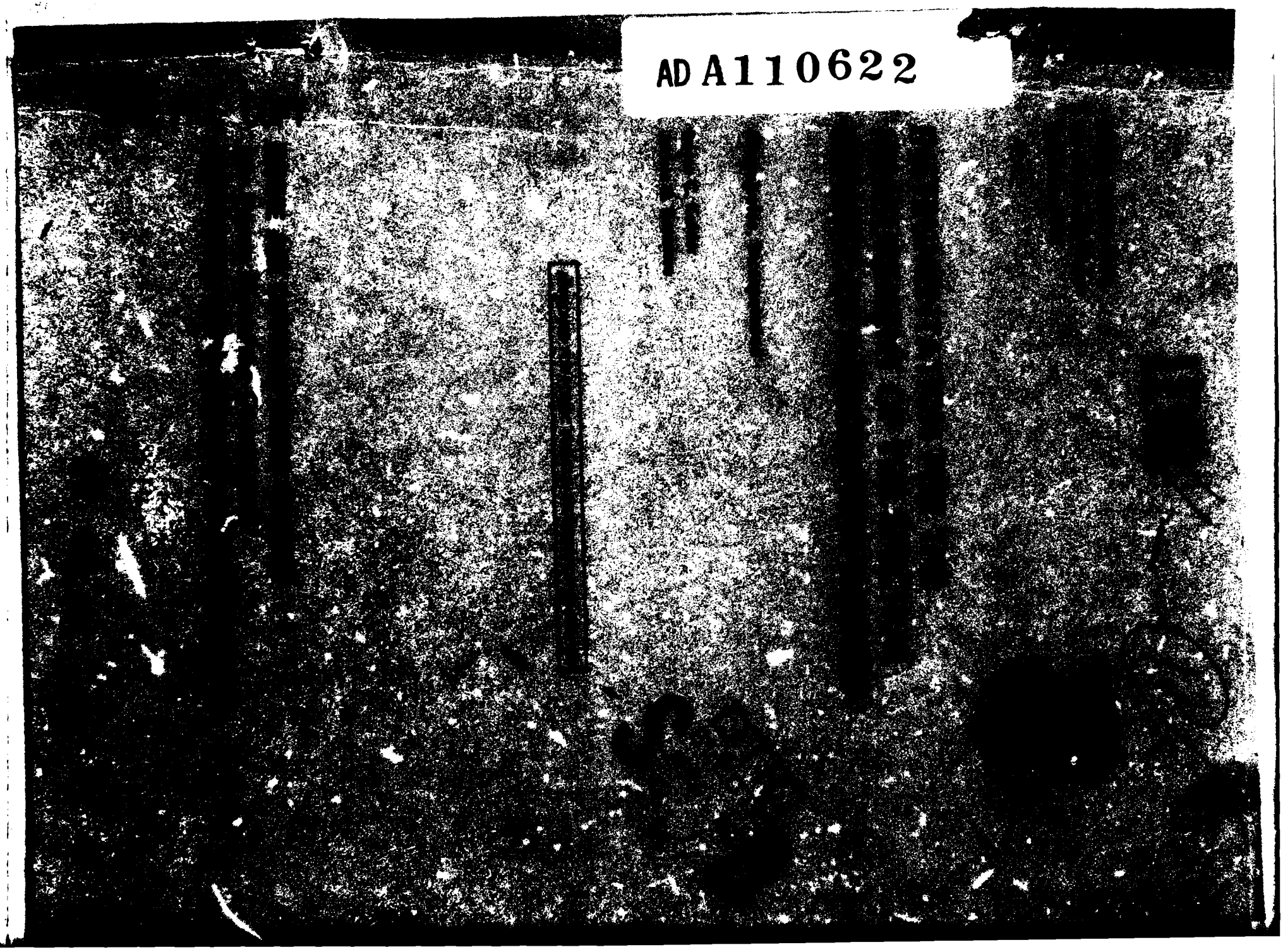
AD A110622

APPROVED:

RICHARD E. MARVIN
Project Engineer

APPROVED:

ALAN G. POWELL
Chief, Electromagnetic Radiation Division

FOR THE COMMANDER:

JOHN P. HUSS
Acting Chief, Plans Office

UNCLASSIFIED

SECURITY CLASSIFICATION OF THIS PAGE (When Data Entered)

REPORT DOCUMENTATION PAGE		READ INSTRUCTIONS BEFORE COMPLETING FORM
1. REPORT NUMBER RADC-TR-81-346	2. GOVT ACCESSION NO. AD-A110	3. RECIPIENT'S CATALOG NUMBER 622
4. TITLE (and Subtitle) INSTRUMENTATION FOR THE MEASUREMENT OF THE SPECTRAL DENSITY OF A RADIATION IMPULSE		5. TYPE OF REPORT & PERIOD COVERED Final Technical Report 6. PERFORMING ORG. REPORT NUMBER N/A
7. AUTHOR(s) Royce C. Kahler James B. Donohoe 61p		8. CONTRACT OR GRANT NUMBER(s) F19628-80-C-0092
9. PERFORMING ORGANIZATION NAME AND ADDRESS Megapulse, Incorporated 8 Preston Court Bedford MA 01730		10. PROGRAM ELEMENT, PROJECT, TASK AREA & WORK UNIT NUMBERS 62702F 46001645
11. CONTROLLING OFFICE NAME AND ADDRESS Deputy for Electronic Technology (RADC/EEP) Hanscom AFB MA 01731		12. REPORT DATE December 1981 13. NUMBER OF PAGES 53
14. MONITORING AGENCY NAME & ADDRESS(if different from Controlling Office) Same 61p.		15. SECURITY CLASS. (of this report) UNCLASSIFIED 15a. DECLASSIFICATION/DOWNGRADING SCHEDULE N/A

16. DISTRIBUTION STATEMENT (of this Report)

Approved for public release; distribution unlimited.

17. DISTRIBUTION STATEMENT (of the abstract entered in Block 20, if different from Report)

Same

18. SUPPLEMENTARY NOTES

RADC Project Engineer: Richard B. Harvey (EEP)

19. KEY WORDS (Continue on reverse side if necessary and identify by block number)

Source Strengths
Sferics
Atmospheric Noise
Spectral Measurement
Receiver Calibration

20. ABSTRACT (Continue on reverse side if necessary and identify by block number)

Natural electrical processes in atmospheric clouds produce individual radio noise impulses of very short duration, as do corona discharges in the air on or near high-voltage conductors. The spectral source-strengths of these impulses are virtually unknown at frequencies above 1 GHz. Besides being of general interest, source-strength information is needed to assess the merits of certain speculative ideas of applications in the fields of lightning hazard avoidance, and passive detection of

DD FORM 1 JAN 73 1473 EDITION OF 1 NOV 65 IS OBSOLETE

UNCLASSIFIED

SECURITY CLASSIFICATION OF THIS PAGE (When Data Entered)

408972

certain missiles.

The source-strength of a radiation impulse can be quantified by measuring its spectral density at some standard distance (e.g. 10 km) from its point of origin. This report describes the equipment, calibrations, field procedures and data reduction methods developed by Megapulse, Incorporated to measure impulse source-strength. The technique was demonstrated by a limited program of 910 MHz cloud-noise measurements at Prospect Hill, Waltham, Massachusetts. Preliminary results are given and compared with the (mostly lower frequency) data reported by other observers. The Megapulse technique could easily be extended to still higher frequencies.

TABLE OF CONTENTS

LIST OF ILLUSTRATIONS

Section 2

Section 3

Section 4

Section 5

LIST OF ILLUSTRATIONS, cont'd

LIST OF TABLES

Section 5

Appendix B

ACKNOWLEDGEMENTS

This program was carried out under contract with the Rome Air Development Center of the United States Air Force. The program was under the general direction of Dr. Peter Ver Planck of Megapulse, Incorporated. Mr. Richard Harvey and Mr. John Heckscher of RADC were project monitors and furnished valuable background information, and certain essential items of equipment. Dr. E.A. Lewis assisted by providing technical consultations. The authors are indebted to Mr. Donald E. Meyers of Megapulse, Incorporated who developed and demonstrated the calibration method used at Prospect Hill.

ABSTRACT

Natural electrical processes in atmospheric clouds produce individual radio noise impulses of very short duration, as do corona discharges in the air on or near high-voltage conductors. The spectral source-strengths of these impulses are virtually unknown at frequencies above 1 GHz. Besides being of general interest, source-strength information is needed to assess the merits of certain speculative ideas of applications in the fields of lightning hazard avoidance, and passive detection of certain missiles.

The source-strength of a radiation impulse can be quantified by measuring its spectral density at some standard distance (e.g. 10 km) from its point of origin. This report describes the equipment, calibrations, field procedures and data reduction methods developed by Megapulse, Incorporated to measure impulse source-strength. The technique was demonstrated by a limited program of 910 MHz cloud-noise measurements at Prospect Hill, Waltham, Massachusetts. Preliminary results are given and compared with the (mostly lower frequency) data reported by other observers. The Megapulse technique could easily be extended to still higher frequencies.

SECTION 1

INTRODUCTION

The peak of the atmospheric noise spectrum is around 10 kHz and is due to radiation from lightning strokes, some of which have currents in the order of 10^5 amperes. The VHF and UHF noise probably has its origin in much smaller currents which may, or may not, be associated with overt lightning flashes. Harvey (1972) used a scanning parabolic antenna to pick up these relatively weak radiations which were then detected by a sensitive threshold-circuit. A two dimensional intensity-modulated cathode ray tube display produced azimuth-elevation "maps" of VHF and UHF electrical activity in clouds. Noise spikes were observed to occur singly, in small groups, and sometimes in large numbers in a burst. The bursts were thought to be associated with lightning flashes, while the small groups were tentatively regarded as indicating an incipient stage of electrification. The single and small-group impulses might possibly provide an advanced warning of conditions hazardous for certain activities such as aircraft refueling, and ammunition handling (Harvey, 1979). In commenting on noise measurements in the USSR, Kachurin (1974) also indicated the possibility of practical applications.

Harvey's experiments (1972) were entirely qualitative; it was found that cloud impulses could be detected at distances of 65 km or more, but source-strengths were not quantitatively established.

Aircraft with jet engines experience radio noise or "precipitation static" even when flying through clear air (Nanevicz, 1970). It appears that due to their differing mobilities, positive and negative ions in the combustion chamber become separated, and a charge builds up on the aircraft. The aircraft has only a small electrical capacity, and its potential rises to the point at which corona discharges occur. At equilibrium, corona carries off the charge as fast as it is produced. The corona current tends to flow from sharp points where the electrical field is larger due to the concentration of field lines. Such points may be found at wing tips, around the stabilizing fins, telemetry stubs, or even at small burrs on the fuselage. Under laboratory simulation conditions, the corona is typically not a steady current, but consists of a series of individual charge-bursts which occur when the air in the immediate vicinity of the point suddenly ionizes, and then more slowly deionizes -- a process which repeats rapidly. The ionization phase occurs very rapidly, and consequently the corona currents have spectral components extending well up into the high radio frequencies. The coupling of these currents to an on-board receiving antenna, or its associated circuitry, injects radio noise into the receiver.

These considerations prompted Lewis (1979) to wonder if the coronal discharges on jet aircraft and jet-propelled missiles might radiate sufficiently to permit detection at useful distances, using high gain directional antennas at UHF frequencies.

The answer to this question depends not only on the electromagnetic source-strength of corona, but on the natural background atmospheric noise. Neither of these factors appears sufficiently well documented to settle such questions with reasonable confidence.

The major objective of the Megapulse work described in this report was to develop and demonstrate equipment and procedures for measuring the source-strength of impulsive noise.

SECTION 2

THEORY OF IMPULSE SPECTRAL SOURCE-STRENGTH SPECIFICATION

The outline of the basic concepts involved in the measurement of spectral source-strength of radio noise impulses as given here follows that of Lewis (1980).

Figure 2.1 illustrates an individual impulse of atmospheric noise incident upon a receiving antenna. Let E(t) represent the time variation of the electrical field (volts m^{-1}) in the polarization to which the antenna responds. The noise impulse causes a voltage transient V(t) to appear across the resistive load R_L of a linear receiver whose effective frequency band pass Δf is centered on frequency f. It is V(t), or some feature of it, that is actually observed.

By Fourier transform theory, E(t) is the sum of sinusoidal fields whose amplitudes and phases vary with frequency:

$$E(t) = \int_0^\infty |\, a(f)\,| \cos(\omega t - \phi)\, df \qquad (2.1)$$

$$= \mathrm{Re} \int_0^\infty a(f) e^{-i\omega t}\, df \qquad (2.2)$$

where $\omega = 2\pi f$, and ϕ is the argument of the complex amplitude spectral density,

$$a(f) = 2 \int_{-\infty}^{\infty} E(t) e^{i\omega t}\, dt \qquad (v\ m^{-1}\ Hz^{-1}) \qquad (2.3)$$

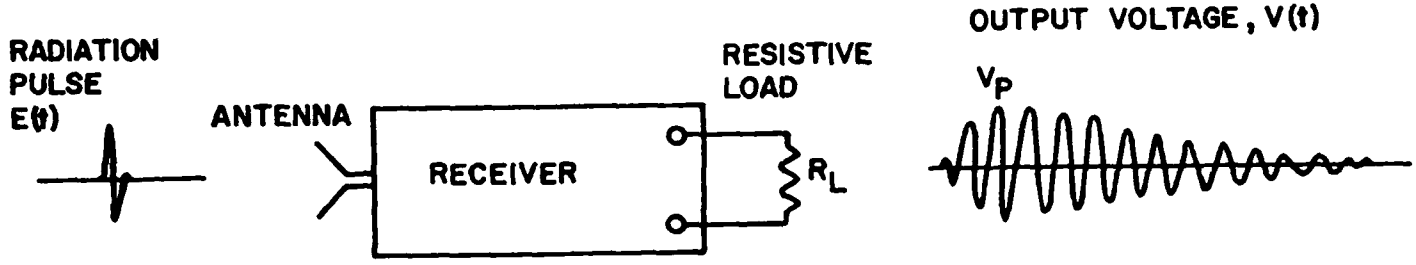

Figure 2.1 Response of a Narrow Frequency Band
Linear Receiver to a Radiation Pulse

The spectral density of the wave-energy incident on a unit area transverse to the direction of propagation (spectral energy intensity) is

$$S'(f) = \frac{|a|^2}{2Z_0} \qquad \text{(joule m}^{-2}\text{ Hz}^{-1}\text{)} \qquad (2.4)$$

assuming a plane wave in essentially free space with $Z_0 = 120\pi$ ohms.

The energy intensity S, in joules per square meter may be found by integrating either with respect to time, or frequency:

$$S = \frac{1}{Z_0}\int_0^\infty E^2(t)dt = \int_0^\infty S'(f)df \qquad (2.5)$$

If A is the absorption cross section of the antenna for the direction from which the impulse is received, and if G is the power gain of the matched receiver, the energy P delivered to the receiver load is $AG\ S'(f)\Delta f$ (joules) provided $S'(f)$ does not vary too much across the pass band Δf. But also

$$P = \frac{1}{R_L}\int_{-\infty}^\infty V^2(t)dt \qquad (2.6)$$

so that

$$S'(f) \approx \frac{1}{AGR_L\Delta f}\int_{-\infty}^\infty V^2(t)dt \qquad (2.7)$$

Thus by observing V(t), or P, the spectral energy intensity S' may be deduced.

If the radiation pulse E(t) is much shorter in duration than the ringing time of the frequency selective networks responsible for the restricted bandwidth Δf, the form of V(t) will be more characteristic of the receiver than of the incident pulse. Then if V_p is the peak of the envelope of V(t)

$$V(t) \approx V_p\, w(t) \tag{2.8}$$

where w(t), an oscillating function of unit peak amplitude, describes the ringing. Then

$$S'(f) = \frac{V_p^2}{AGR_L \Delta f} \int_{-\infty}^{\infty} w^2(t)\,dt \tag{2.9}$$

and

$$|a(f)| = V_p \sqrt{\frac{2Z_\theta}{AGR_L \Delta f} \int_{-\infty}^{\infty} w^2(t)\,dt} \tag{2.10}$$

As a practical procedure, the coefficient of V_p in Equation (2.10) may be measured by means of a calibrating impulse of known spectral value. However, even if the value of this integral is not measured, a rough estimate may be made from fundamental considerations which suggest the effective duration of w(t) is in the order of $(\Delta f)^{-1}$. It is then reasonable to expect the integral to be in

the order of $(4\Delta f)^{-1}$ seconds. A more detailed analysis by Horner (1964) suggests that $(2\sqrt{2}\,\Delta f)^{-1}$ is a better value to use with multi-stage band pass circuits. Then

$$S'(f) \approx \frac{V_p^2}{2\sqrt{2}\,AGR_L(\Delta f)^2} \tag{2.11}$$

and hence

$$|a(f)| \approx \frac{V_p}{\Delta f}\sqrt{\frac{Z_o}{2AGR_L}} \tag{2.12}$$

For a receiving antenna on the ground, an elevated noise-source, and an uneven, vegetated earth surface, it probably suffices at least for preliminary studies, to assume that the ground-reflected wave may be neglected. The propagation is then essentially line-of-sight, and it follows that the impulse, and the spectral amplitude $a(f)$, are inversely proportional to the slant range. If, as will be the case here, 10 km is adopted as a standard reference distance, then the amplitudes of sources nearer or farther than 10 km may be adjusted accordingly.

In the observation of a noise impulse from a cloud there are a number of unknown factors including: the directional pattern of the source, the pattern orientation with respect to the direction of the receiving antenna, the source polarization, and even the exact propagation distance. These variable and uncontrolled elements in the measurements prevent the specification of source-strength simply in Joules per Hertz. For a simple source-model

consisting of an infinitesmal dipole of random orientation, a calculation shows that the average field-strength is about 79% of the maximum. Similarly, for a given field-strength and random polarization, the average effective field-strength is about 64% of the maximum. Also some sources will not be in the direction of maximum antenna gain. These factors, plus any natural variability from one source to another, may be expected to cause a noticeable spread in measured values of $a(f)$.

SECTION 3

RECEIVING AND RECORDING EQUIPMENT

A block diagram of the receiving equipment is shown in Figure 3.1. The antenna, provided by R. B. Harvey, was a four-element, one-meter "back-fire" type based on designs of Ehrenspeck and Strom, and chosen for its very low back lobes (Strom, 1974). Figure 3.2 and 3.3 are pictures of the antenna and its enclosure at Prospect Hill. The antenna gain, measured on an Air Force test range, was 19 dB over isotropic at 920 MHz, corresponding to an absorption cross-section of 0.7 m^2. Figure 3.4 shows the azimuthal antenna pattern, and the elevation pattern was similar. The nominal beamwidth was 20°, and the frequency bandwidth was 40 MHz centered on 910 MHz. The antenna was mounted so as to respond to radiation with "vertical" electric, or TM polarization.

The antenna mount and drive (manufactured by Rotating Precision Mechanism), permitted 360° of continuous azimuthal rotation, and from -10° to +90° of elevation. The direction of the antenna was shown by azimuth and elevation dials on the antenna drive unit. A synchro-to-analog converter coupled to the azimuth dial was used to generate the sweep direction on the (Tektronix 603) display oscilloscope (see Figure 3.1 and the discussion below).

Following the antenna was a Telonic Model TCN 910-40 coaxial cavity filter also with a bandwidth of 40 MHz at 910 MHz. Following this was an Avantek Model AK 1000N preamplifier with broad

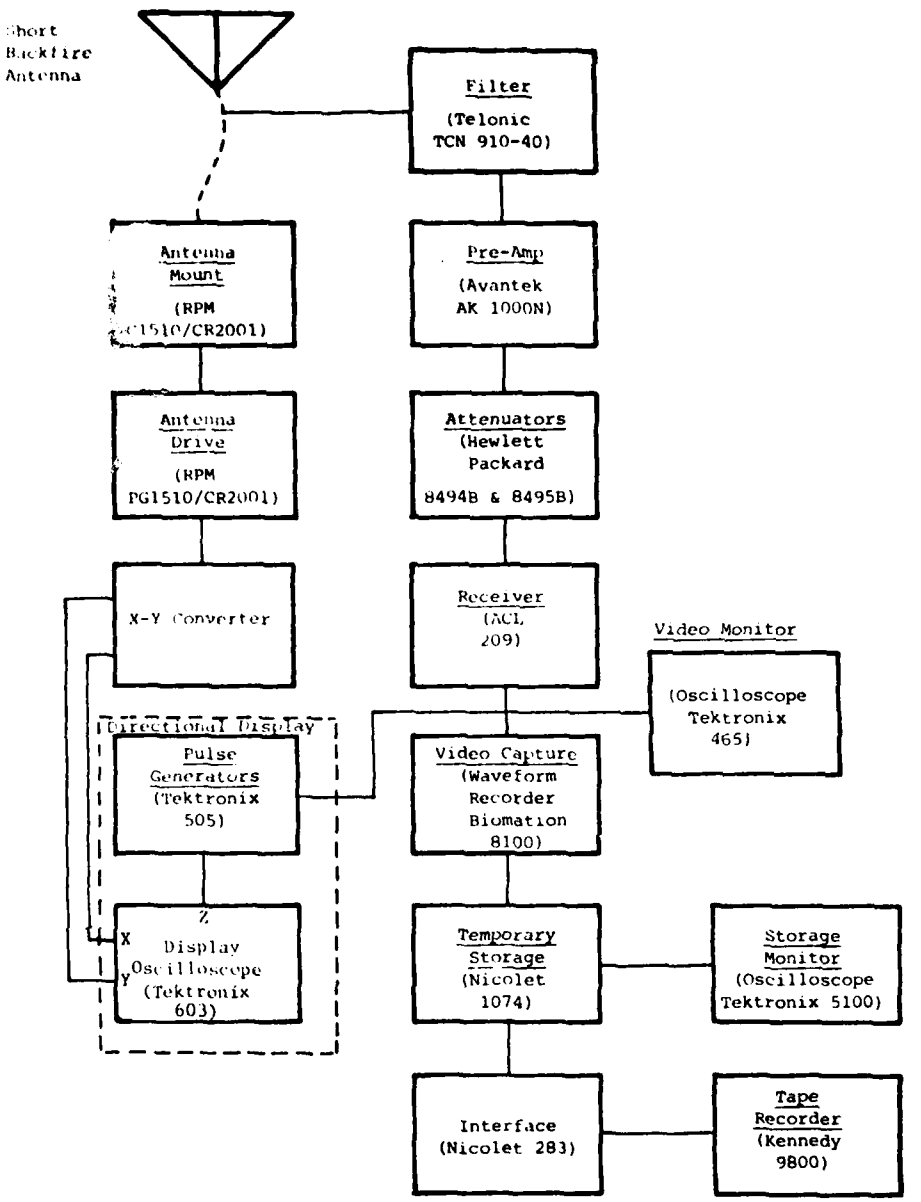

Figure 3.1 Block Diagram of Receiving Equipment.

Figure 3.2 (Top) Backfire Antenna, Enclosure Partially Open.

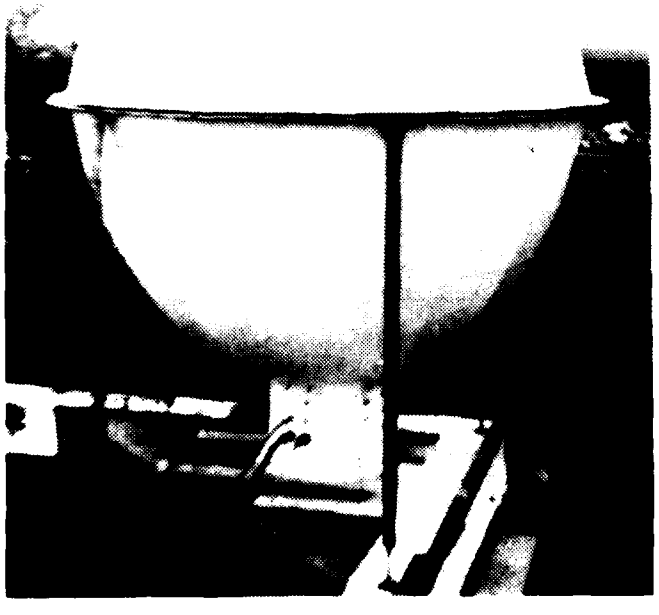

Figure 3.3 (Left) Fiberglass Antenna Enclosure.

Figure 3.4 Azimuthal Antenna Pattern

band (500 to 1000 MHz) and low noise (3 dB noise figure). This preamplifier drove a 15 meter-long double shielded coaxial cable (RG-9) running down to a building.

Inside the building, the cable terminated in attenuators (Hewlett-Packard Models 8494B and 8495B) with a combined range of 0 to 81 dB in steps of one dB, good from DC to 18 GHz. In measuring the RF impulses, these attenuators provided the only gain adjustments used: the response to the following equipment remained constant.

Following the RF attenuators, was a double superheterodyne receiver (ACL Model 209) with 60 MHz and 21 MHz IF's , the latter having a 3 MHz bandwidth. This was followed by a linear detector giving a video output which could be monitored by a Tektronix Model 465 oscilloscope. This video output is essentially the envelope of the "ringing function" V(t) of Equation (2.8). The video output also went to a directional display unit consisting of a Tektronix 505 Pulse Generator and a storage oscilloscope (Tektronix 603). When the video pulse amplitude exceeds the triggering threshold of the 505, a 6 μsec pulse was generated to momentarily intensify the beam of the 603 oscilloscope, producing a bright dot, and to start a 20 millisecond sweep (if it had not already been started by a previous pulse). The sweep started at the center of the screen, and went radially outwards in a direction corresponding to the azimuth in which the antenna was pointing. As the antenna swept around the horizon the sweep direction

rotated creating a "wagon-wheel" display. The rotating sweep was accomplished by a "sine/cosine" converter electrically locked to the antenna drive. Threshold-exceeding pulses, following within 20 milliseconds of the one which started the sweep, appeared as bright dots along the line of sweep. Thus for example, a fixed source of time-random noise impulses located due west of the antenna would appear as a fan-shaped distribution of dots in a sector corresponding to the effective beamwidth of the antenna somewhat as illustrated in Figure 3.5. The storage feature of the oscilloscope allowed the dots to accumulate until erased by the operator. If desired, a permanent record was made by photographing the display with a frame camera.

For preserving the 'video' information in quantitative form, the output of the ACL 209 receiver went to a Biomation Model 8100 Waveform Recorder. This device has a 2048 word memory, and an 8 bit analog-to-digital converter with sampling intervals as short as 10 nanoseconds (it was found that 20 ns was adequate). On command, the contents of the memory were transferred at a slower rate to a Nicolet 1074 Signal Averager which provided temporary storage of the captured 'video' information. The Nicolet unit has a rotating memory so that the stored 'video' could be recovered through a digital-to-analog converter for continuous viewing on an oscilloscope (Tektronix Model 5100). The Nicolet memory could be stored permanently, in digital form, on magnetic tape. The tape recorder (Kennedy Model 9800) had nine tracks, and used standard

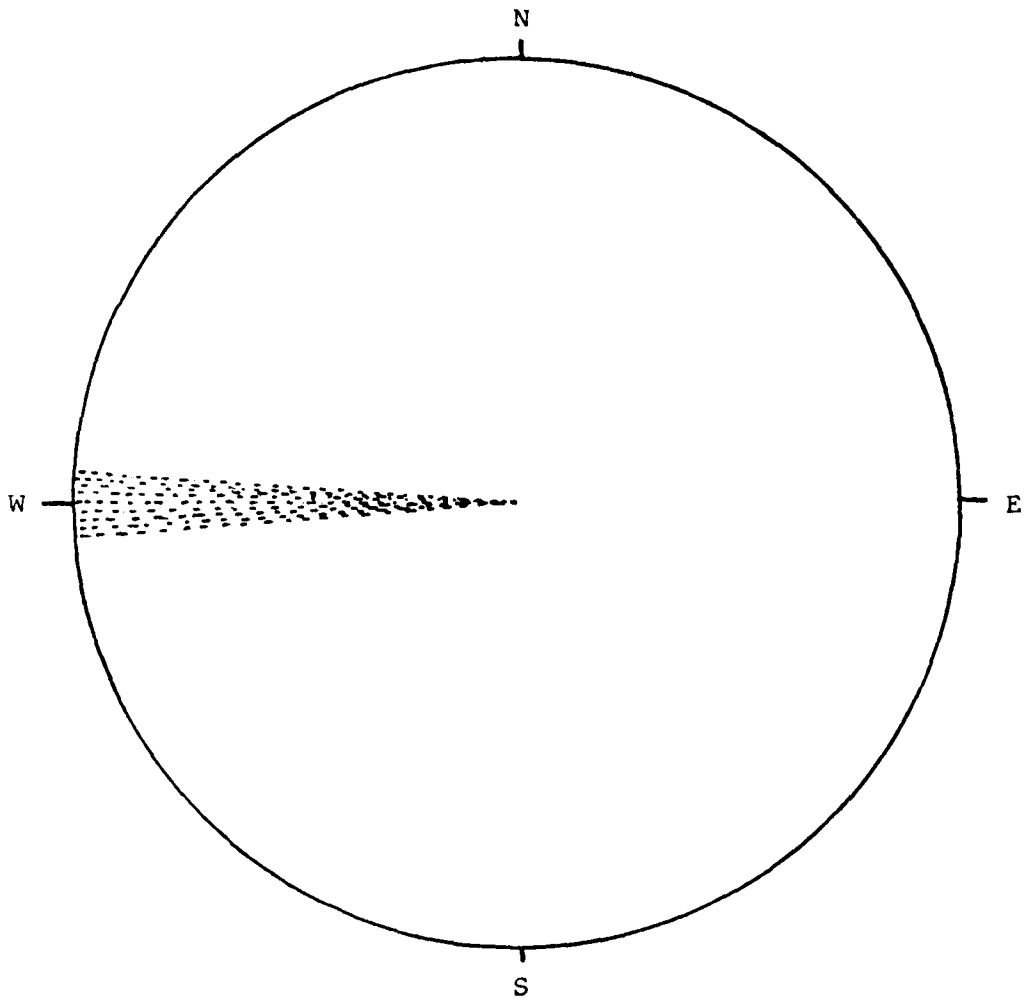

Figure 3.5 Fan-like CRT Display of Random Impulses from a Point Source Due West of the Antenna.

400 meter (1200 foot) reels. Approximately 720 records could be recorded about 2 seconds apart. A Nicolet Model 283 provided the interface between the temporary storage and the tape machine. Tape recorded data could be recovered in graphical form by playing the tape back through the Nicolet Model 1074, to an X/Y Plotter (Hewlett-Packard Model 7046A).

SECTION 4

CALIBRATION

In its simplest form, calibration would consist of disconnecting the coaxial cable from the antenna, and connecting it directly to an impedance-matched generator of voltage impulses of known spectral content. The amplitudes and shapes of the resulting video impulses, recorded on magnetic tape provided the basis for a direct quantitative comparison with the video pulses from the noise sources. Inspection of the shape of the video pulses permits the analyst to verify that the durations of the noise impulses were indeed much shorter than the ringing time of the frequency selective circuits (receiver bandwidth of 3 MHz), and hence satisfy the assumption on which Equations (2.8) through (2.12) rest. It is noted that for a given spectral content, shorter pulses must have a greater amplitude, and hence require a greater range of linearity in the electronic equipment.

In this method of calibration the essential factors are antenna absorption cross section, spectral content of the calibration pulse and the RF attenuators preceding the receiver. The calibration pulse generator was a Singer Model 91263-1 which produced a "box-car" voltage impulse only about 5×10^{-10} seconds in duration. This impulse and its spectral content are discussed in Appendix A.

Figure 4.1 shows the shape of the 'video' transient produced by a calibration pulse. The amplitude of the 'video' transient was linearly proportional to the voltage of the "box-car".

In routine practice the calibration pulse was not injected directly into the cable. Instead, it was radiated into the back-fire antenna from a quarter wave monopole set up at a fixed distance (see Appendix A).

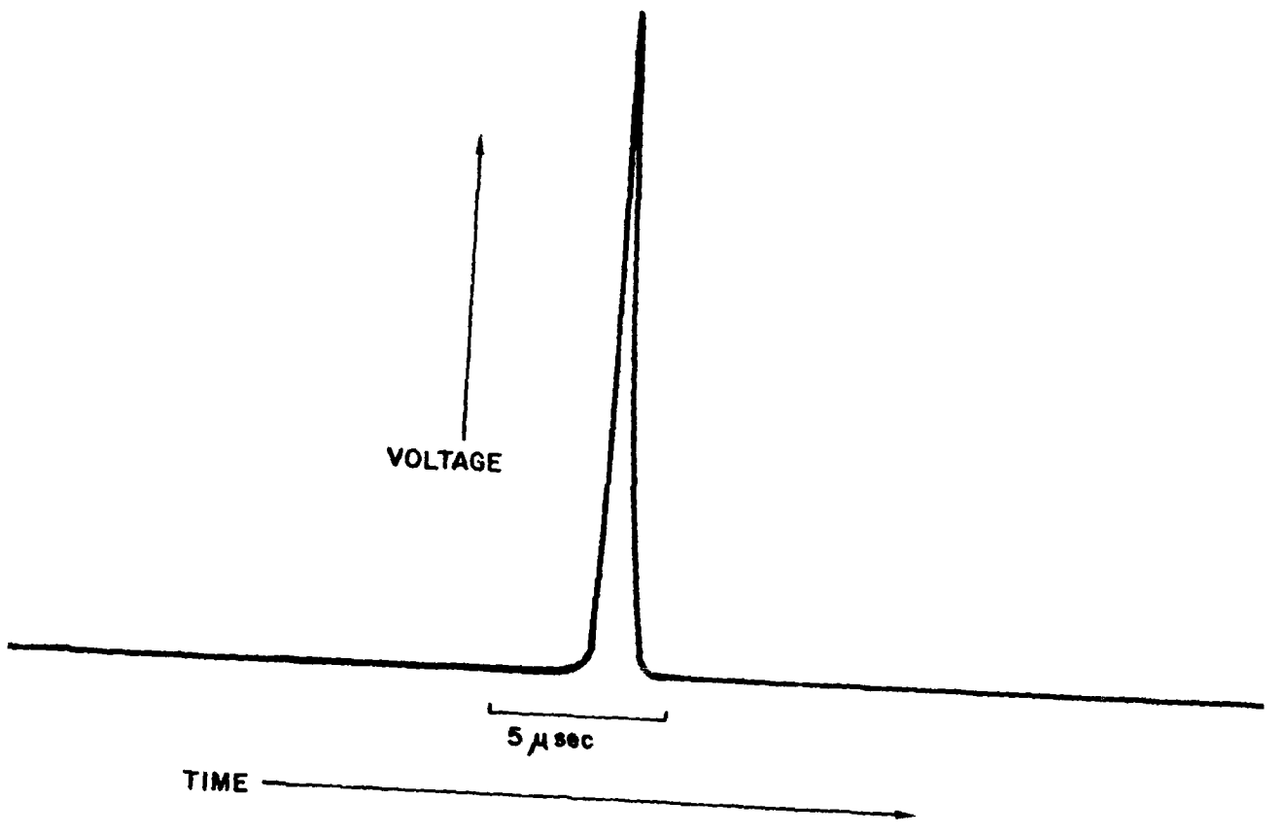

Figure 4.1 Typical "Video" Waveform Produced by R.F. Calibration Pulse.

SECTION 5

CLOUD-NOISE MEASUREMENTS

To demonstrate the use of the impulse-measuring equipment, recordings were made of impulses from clouds in the vicinity of the Prospect Hill receiving site. The approximate distances to the clouds generating the impulses were determined by means of weather radar range-azimuth pictures from the National Oceanographic and Atmospheric Administration (NOAA) station at Chatham, Massachusetts which is about 132 km from Prospect Hill, see Figure 5.1. The location of Prospect Hill is also indicated on the radar pictures, Figures 5.2 through 5.7. These figures show precipitation regions as dark areas, not all of which were necessarily sources of impulse noise. However, local weather reports from radio and television stations together with the directional distribution of the impulse noise shown on the directional display integral to the receiving equipment itself (refer to Section 3 of this report) sometimes allowed the precipitation areas responsible for the noise to be identified with high probability. Although the ideal situation -- just one small, but electrically active, precipitation cell in the whole coverage area -- did not occur during the demonstration period, there were three cases in which the source locations were considered reliable. These are shown as S1, S2 and S3 in Figure 5.1 and elsewhere. These sources remained

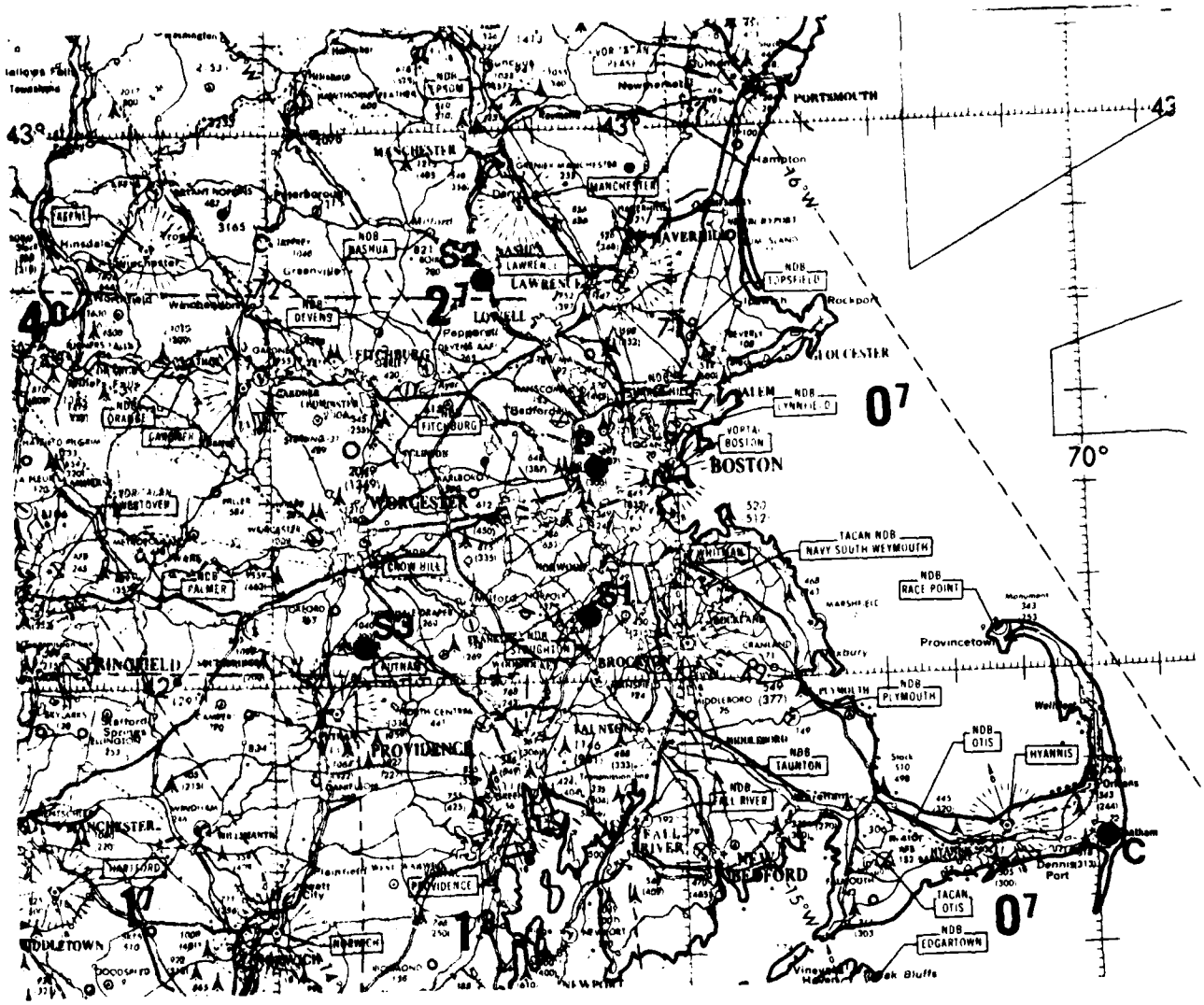

C - Chatham (Radar)
P - Prospect Hill (Receiving Site)
S1 - Storm 22.30-23.00, 4 Aug 1980
S2 - Storm 20.18-20.38, 6 Aug 1980
S3 - Storm 22.26-22.42, 6 Aug 1981

(GMT)

Figure 5.1 Map of Eastern Massachusetts Showing Locations.

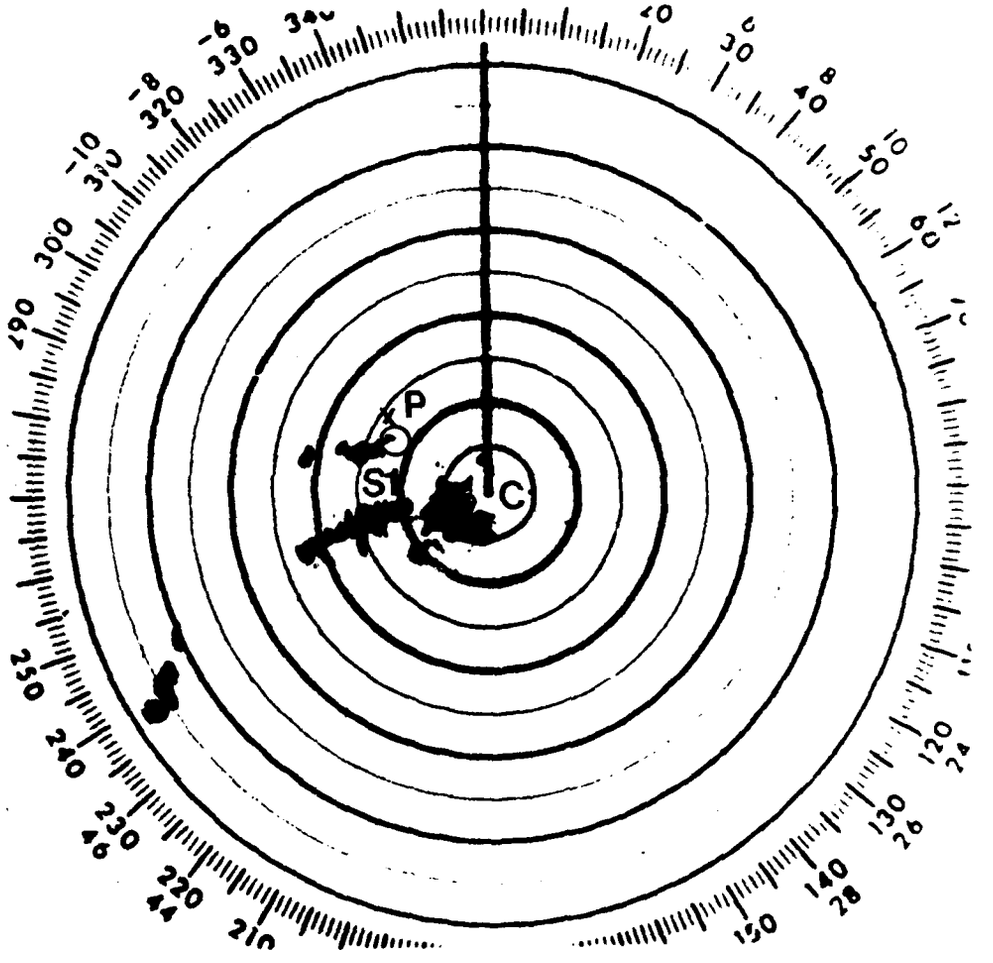

Outer Range-circle: 250 naut. mi. (463 km)

Point P: Prospect Hill

Point ◯: Probable Source of Impulses.

Time: 22.29 GMT, 4 August 1980.

Figure 5.2 Radar Picture Early in the Development of Source S1.

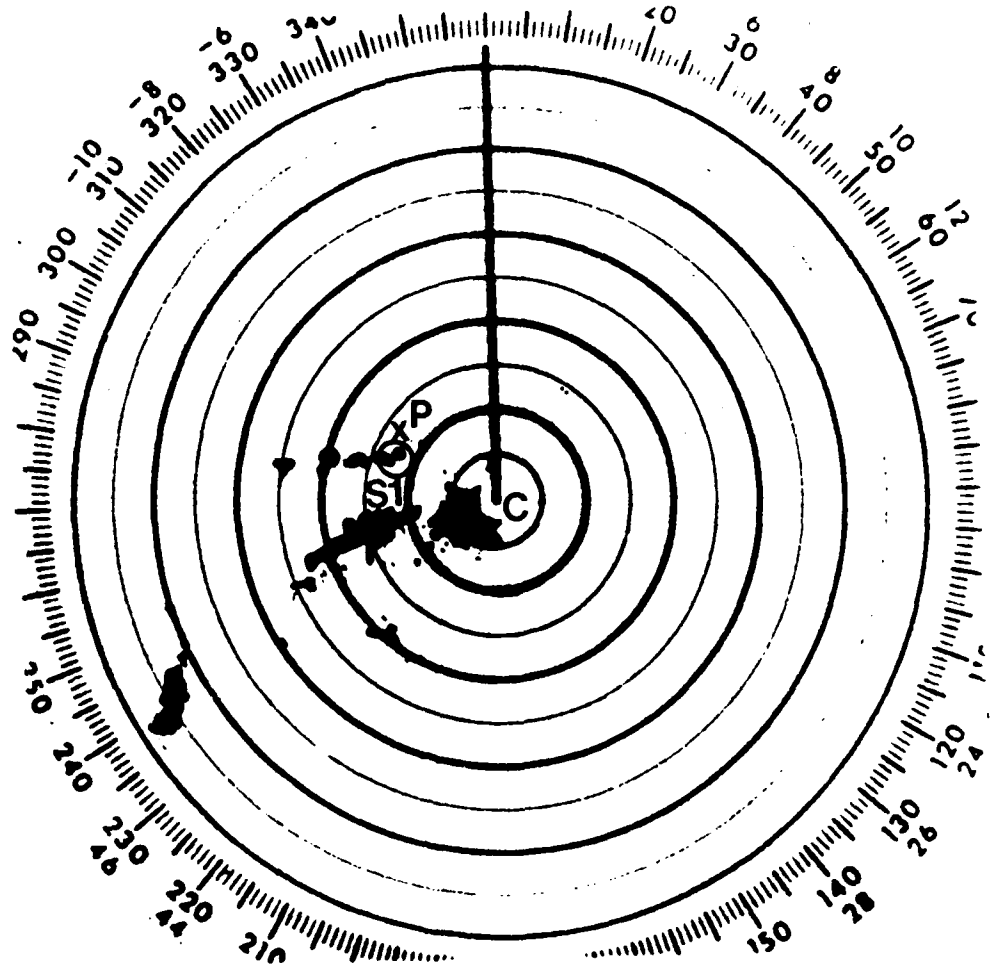

Outer Range-circle: 250 naut. mi. (463 km)

Point P: Prospect Hill

Point ◯ : Probable Source of Impulses.

Time: 22.56 GMT, 4 August 1980.

Figure 5.3 Radar Picture Late in the Development of Source S1.

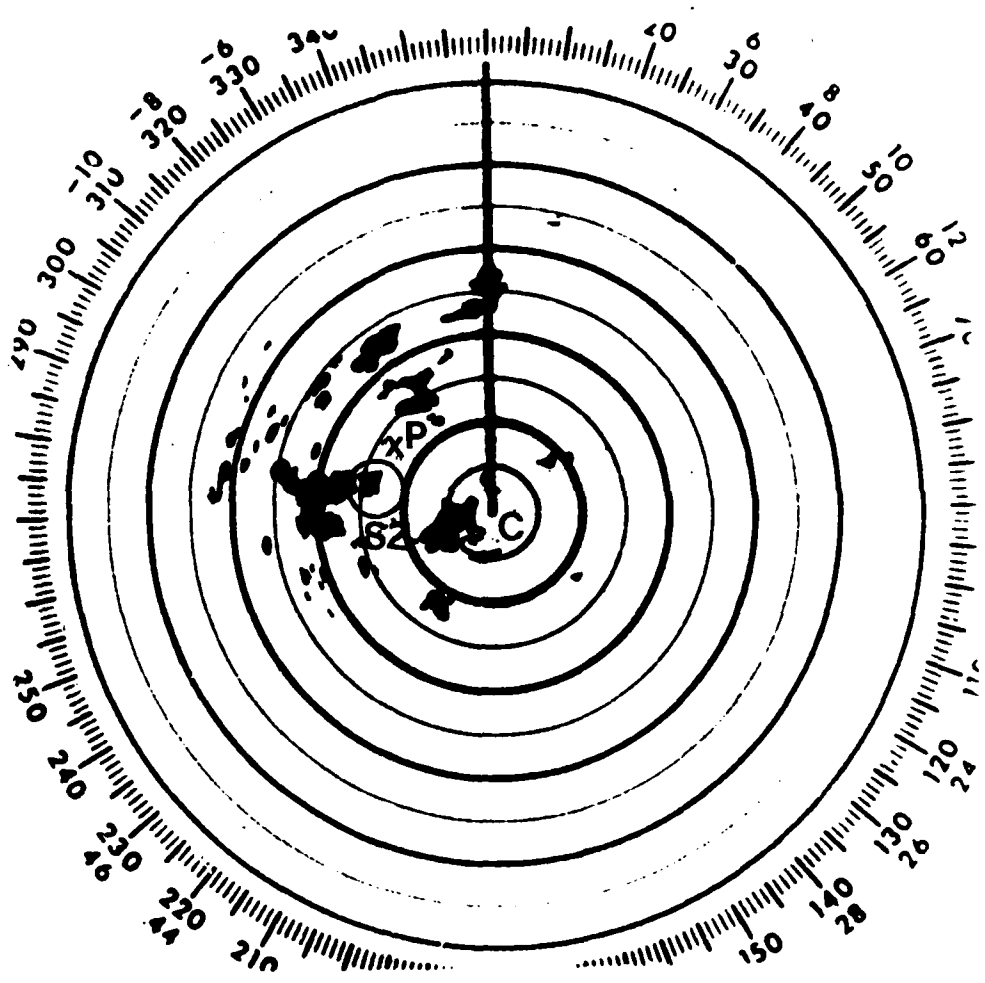

Outer Range-circle: 250 naut. mi. (463 km)

Point P: Prospect Hill

Point ◯ : Probable Source of Impulses.

Time: 20.17 GMT, 6 August 1980.

Figure 5.4 Radar Picture Early in the Development of Source S2.

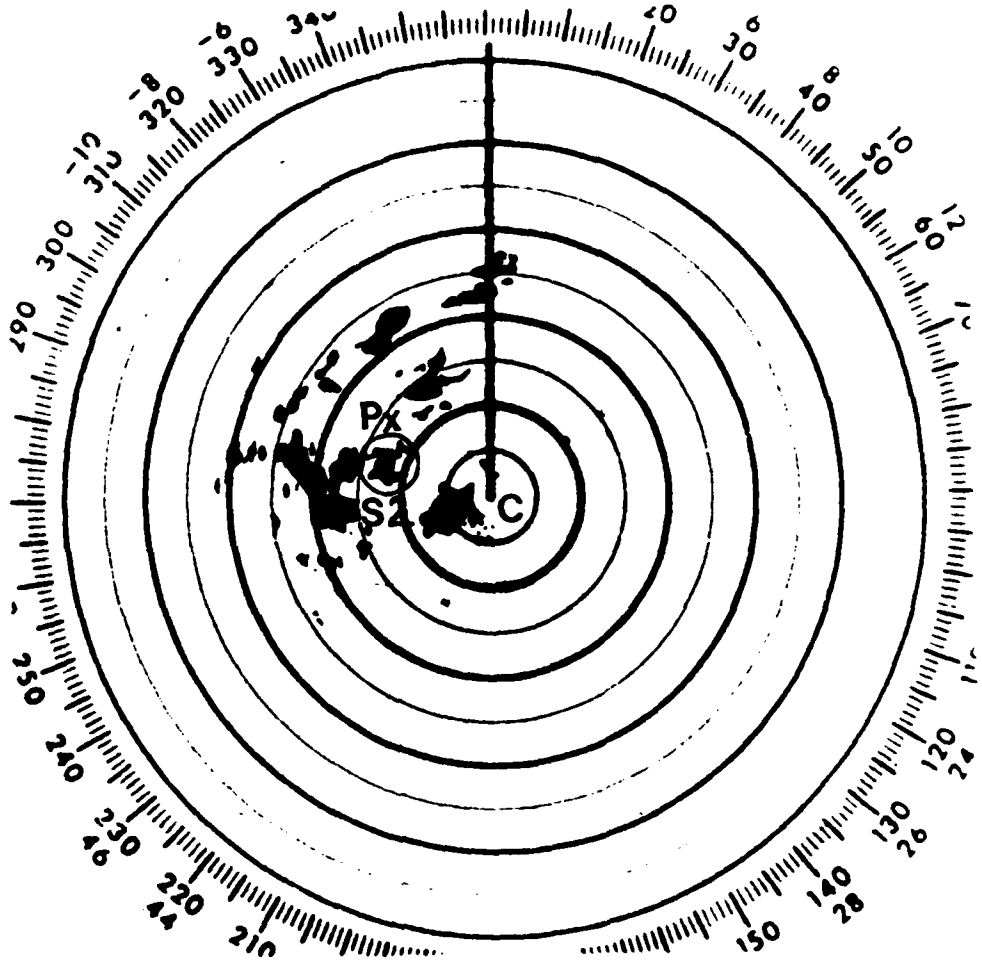

Outer Range-circle: 250 naut. mi. (463 km)

Point P: Prospect Hill

Point ◯ : Probable Source of Impulses

Time: 20.38 GMT, 6 August 1980.

Figure 5.5 Radar Picture Late in the Development of Source S2.

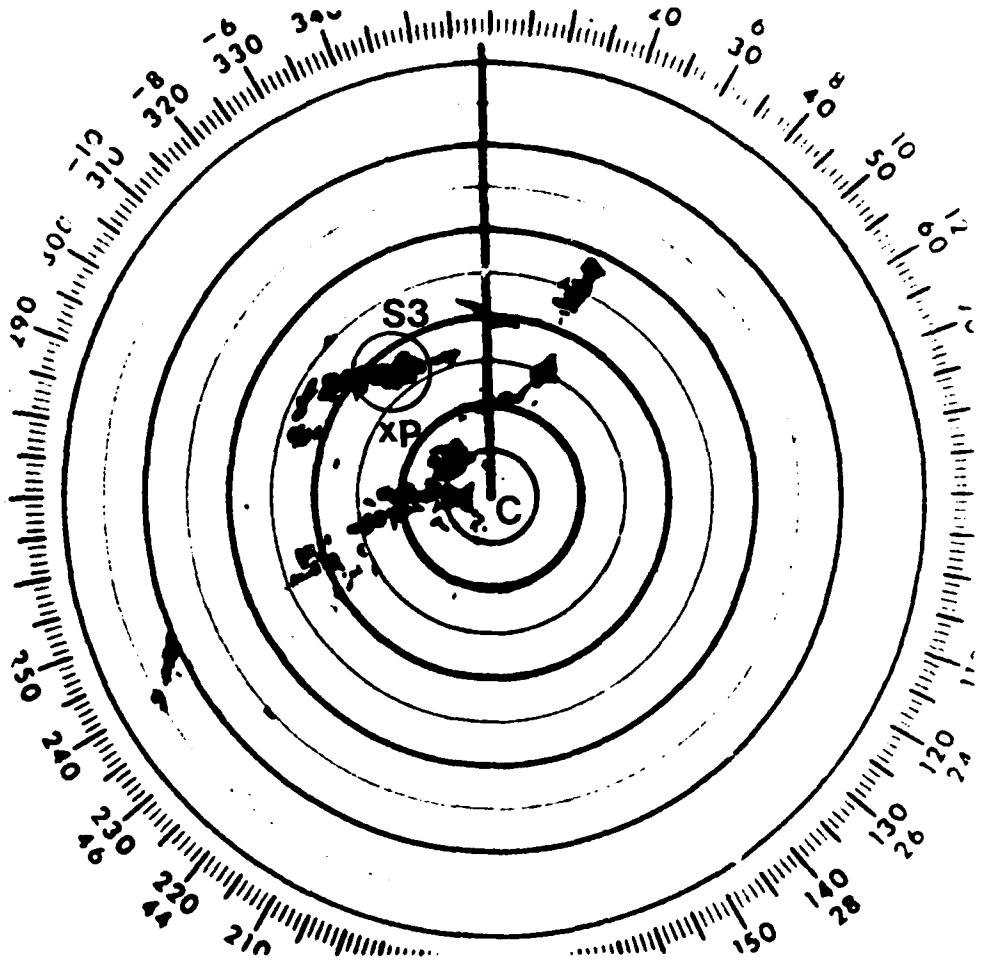

Outer Range-circle: 250 naut. mi. (463 km)

Point P: Prospect Hill

Point ◯ : Probable Source of Impulses.

Time: 22.26 GMT, 6 August 1980.

Figure 5.6 Radar Picture Early in the Development of Source S3.

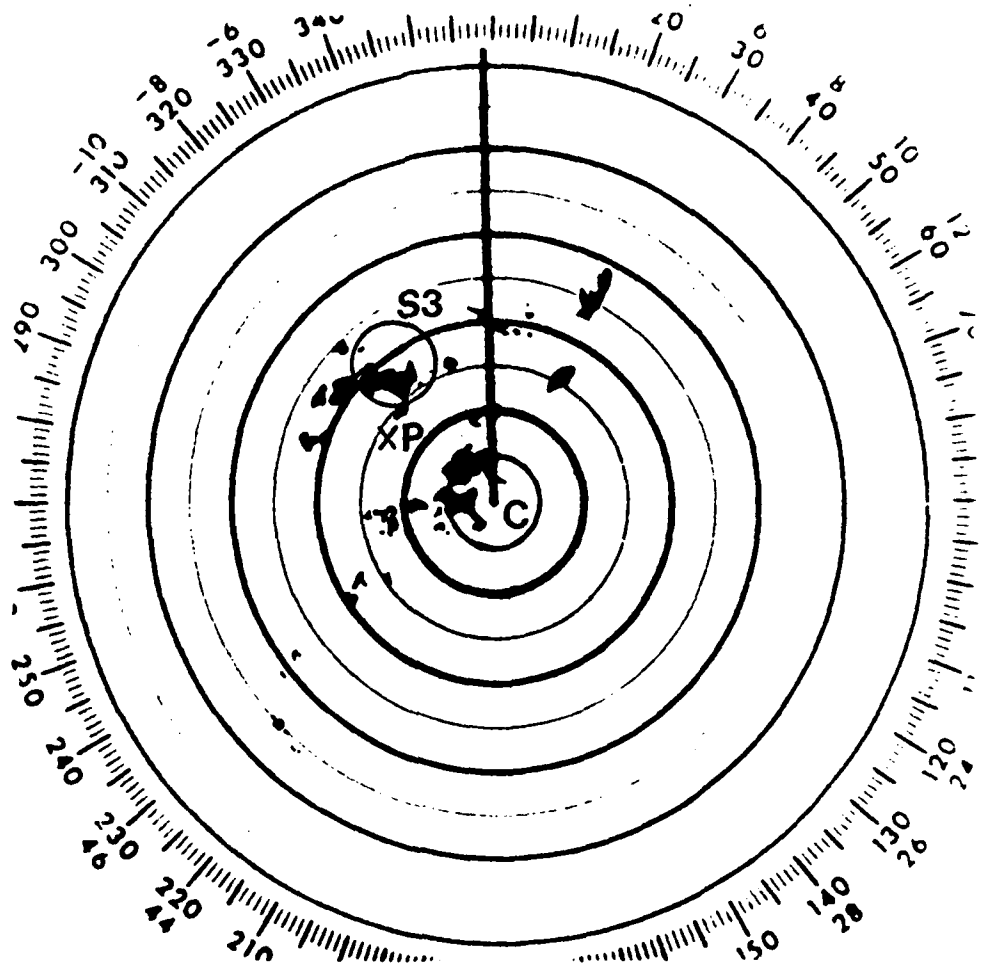

Outer Range-circle: 250 naut. mi. (463 km)

Point P: Propsect Hill

Point ◯: Probable Source of Impulses.

Time: 22.42 GMT, 6 August 1980.

Figure 5.7 Radar Picture Late in the Development of Source S3.

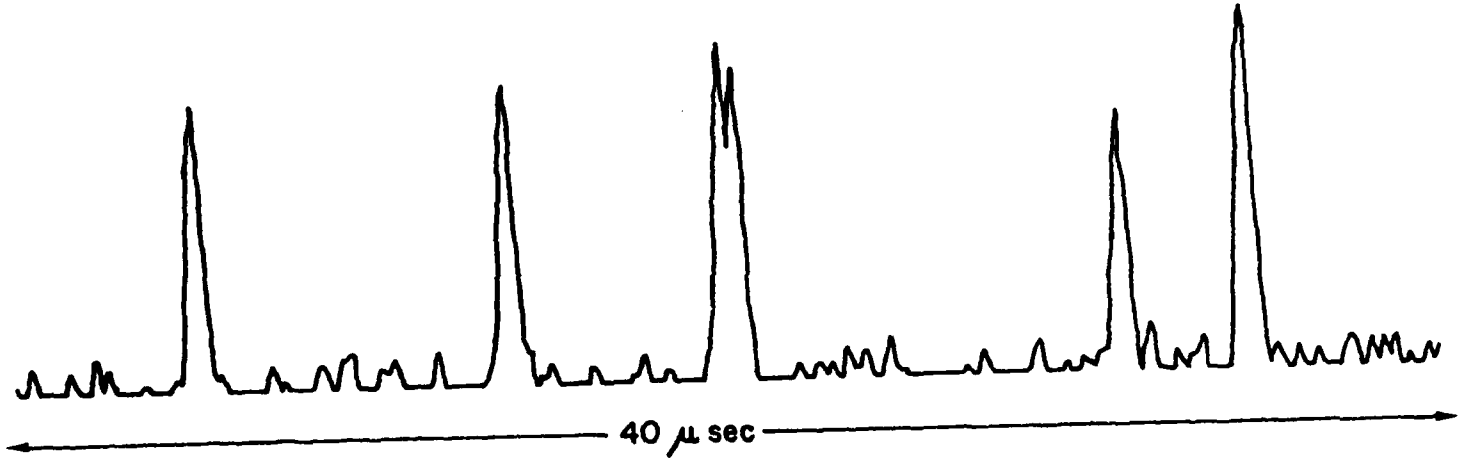

Figure 5.8 Sample of Pulses Received During Storm Si.

active for a half-hour or so, and in Figures 5.2 through 5.7 two radar pictures are given for each case (one taken early in the source development and the other taken later). The radar pictures were reproduced from 16 mm file records supplied by the NOAA.

Tape recorded impulses from S1, S2 and S3 were converted to hard copy form by means of an X/Y plotter. Figure 5.8 shows a sample of the data containing five impulses. The third impulse has a double peak and greater width than the others, features which indicate that there were two RF impulses too close together to be completely resolved. In such cases (refer also to Section 6 of this report) amplitude measurements were not made, although the amplitude of the first peak of the double impulse in Figure 5.8 for example could be considered valid with high confidence.

Spectral densities for individual impulses from S1, S2 and S3 were obtained, and adjusted to the standard 10 km distance, with the results shown in Tables 5.1, 5.2 and 5.3 respectively. Table 5.4 summarizes these data.

Table 5.1 Storm S1 Spectral Densities Normalized to 10km.

Pulse No.	Time GMT.	Spectral Density $\|a\|$ (Volts. Meter^{-1}Hertz^{-1})
1	2230	25×10^{-10}
2	2231	33
3	2232	28
4	2234	20
5	2235	18
6	2235	18
7	2235	25
8	2236	18
9	2236	18
10	2237	18
11	2237	18
12	2238	20
13	2239	20
14	2240	38
15	2241	18
16	2241	25
17	2242	30
18	2243	28
19	2244	18
20	2245	25
21	2248	28
22	2251	18
23	2251	18
24	2252	28
25	2253	18
26	2254	18
27	2255	18
28	2256	23
29	2257	18
30	2258	18
31	2259	18
32	2300	18

Table 5.2 Storm S2 Spectral Densities Normalized to 10km.

Pulse	Spectral Density $\|a\|$ (Volts. Meter^{-1} Hertz^{-1})	Pulse	Spectral Density $\|a\|$ (Volts. Meter^{-1} Hertz^{-1})	Pulse	Spectral Density $\|a\|$ (Volts. Meter^{-1} Hertz^{-1})
1	9.0×10^{-10}	30	9.0×10^{-10}	59	9.8×10^{-10}
2	8.3	31	10.5	60	8.5
3	9.3	32	9.0	61	8.3
4	7.8	33	8.3	62	8.5
5	8.5	34	9.3	63	10.0
6	3.0	35	8.8	64	10.5
7	8.0	36	10.5	65	11.5
8	10.5	37	11.3	66	7.5
9	9.3	38	8.8	67	9.0
10	7.8	39	9.0	68	8.5
11	8.0	40	8.8	69	9.3
12	9.0	41	11.3	70	10.8
13	8.3	42	10.0	71	9.3
14	10.0	43	10.5	72	10.3
15	11.3	44	10.0	73	11.3
16	11.3	45	10.8	74	8.5
17	11.3	46	9.5	75	8.3
18	8.0	47	9.8	76	10.0
19	8.8	48	8.8	77	10.8
20	10.3	49	10.5	78	11.3
21	9.5	50	10.5	79	9.0
22	8.3	51	10.3	80	9.3
23	8.3	52	10.0	81	9.8
24	11.3	53	9.5	82	2.8
25	9.5	54	8.8	83	9.0
26	9.5	55	8.3	84	9.8
27	9.5	56	10.8	85	10.0
28	10.8	57	9.3	86	10.5
29	10.8	58	11.3		

Table 5.3 Storm S3 Spectral Densities Normalized to 10km.

Pulse	Spectral Density $\|\underline{a}\|$ (Volts. Meter^{-1}Hertz^{-1})	Pulse	Spectral Density $\|\underline{a}\|$ (Volts. Meter^{-1}Hertz^{-1})
1	6.0×10^{-10}	30	5.3×10^{-10}
2	6.5	31	5.0
3	5.3	32	5.0
4	6.5	33	4.8
5	6.5	34	4.8
6	6.0	35	4.8
7	6.3	36	4.5
8	5.3	37	6.0
9	6.5	38	2.8
10	5.0	39	6.0
11	6.5		
12	6.5		
13	6.5		
14	5.8		
15	5.8		
16	6.3		
17	6.5		
18	4.5		
19	6.0		
20	4.5		
21	4.8		
22	4.5		
23	5.8		
24	6.0		
25	6.0		
26	5.0		
27	6.0		
28	5.3		
29	6.5		

Table 5.4 Cloud - Noise Data Summary

Storm	Approx. Distance from Prospect Hill	Number of Impulses Analysed	Average Spectral Density |a| Normalized to 10 km	RMS Deviation
S_1	29 km	32	22×10^{-10} vm^{-1} Hz^{-1}	7.7×10^{-10} vm^{-1} Hz^{-1}
S_2	48	86	2.5×10^{-10}	1.6×10^{-10}
S_3	60	39	5.6×10^{-10}	0.68×10^{-10}
	Total	157	Average: 12×10^{-10} vm^{-1} Hz^{-1}	

SECTION 6

DISCUSSION

The average spectral density for all three storms (from Table 5.4) is shown in Figure 6.1 as a point added to a data plot derived from information published by other workers (Lewis, 1981). The published data at frequencies above 300 MHz has a spread of at least a factor of 10, and the Megapulse point based on 157 impulses is reasonably consistent with the other data.

From Table 5.4 it appears that the more distant storms gave weaker source-strengths, but this may be coincidental. A much larger data base would be needed to investigate this.

While the spread of data shown in Figure 6.1 makes any extrapolation to frequencies above 1 GHz very doubtful, the stage is now set for exploring this unknown region. The Megapulse equipment could readily be adapted to this purpose by substituting a higher frequency receiver and RF components. (A horn antenna suitable for the 2 to 4 GHz range was obtained, but was not used in the present program.)

Some qualitative comments about the nature of the cloud-noise observed at 910 MHz may be of interest. Figure 6.2 shows reproductions of two Polaroid photographs of the display on the video monitor oscilloscope (Tektronix 465, see Figure 3.1). These oscillograms illustrate typical impulse sequences associated with visible lightning flashes in the vicinity of Prospect Hill. In

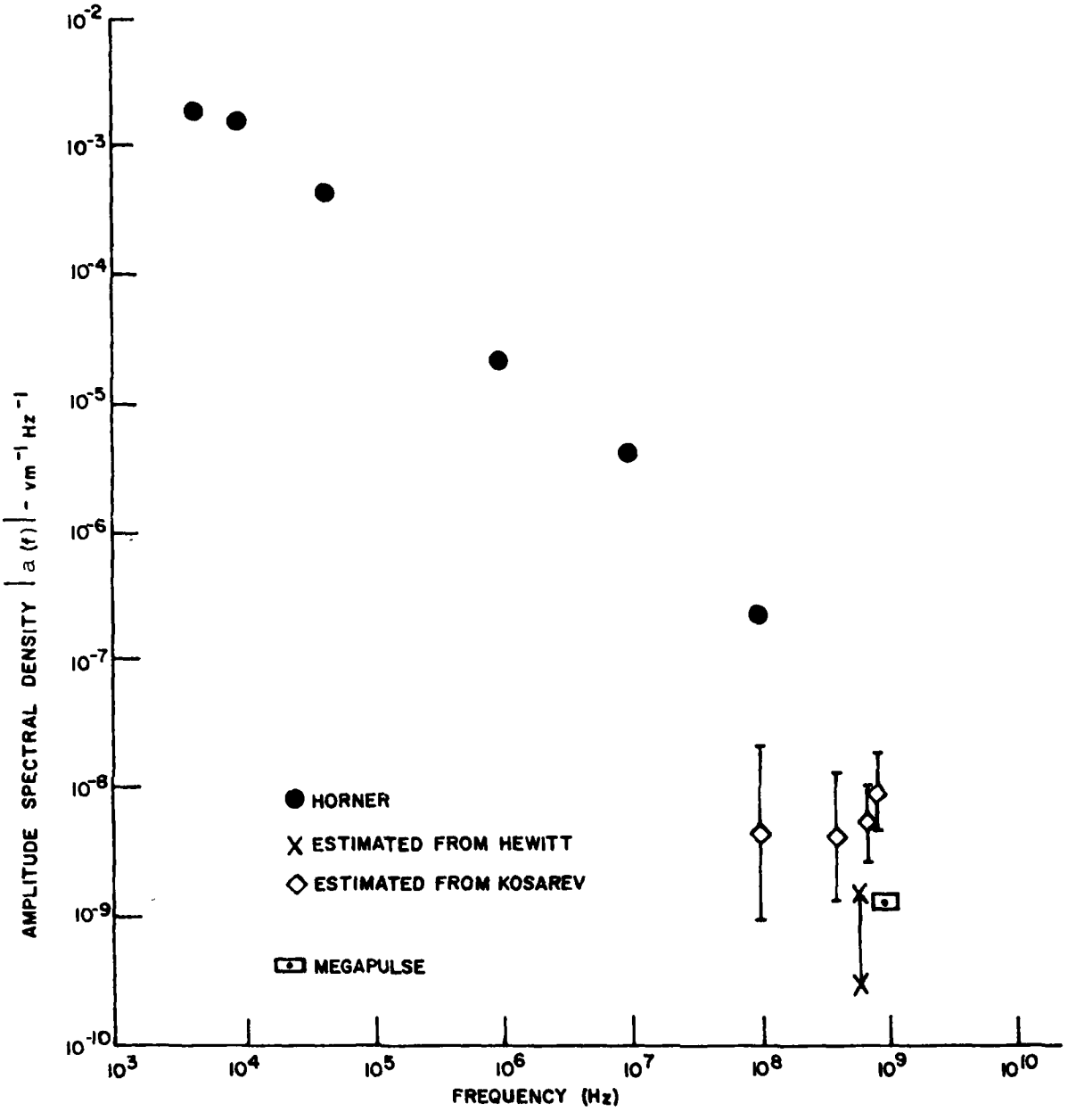

Figure 6.1 Amplitude Spectral Density of Sferics Normalized to 10 km Distance

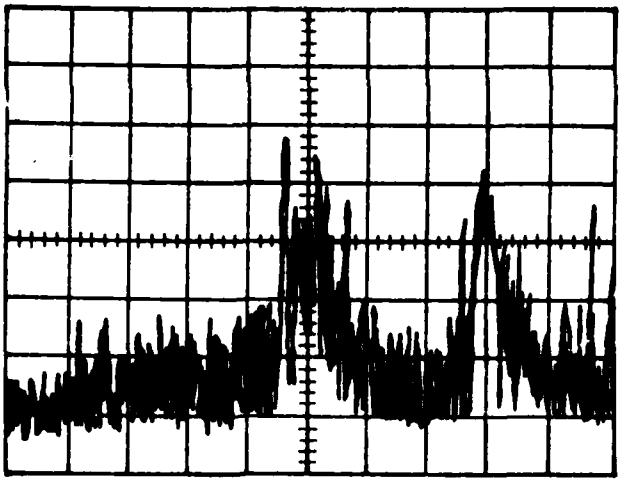

20 MICROSECONDS PER DIVISION

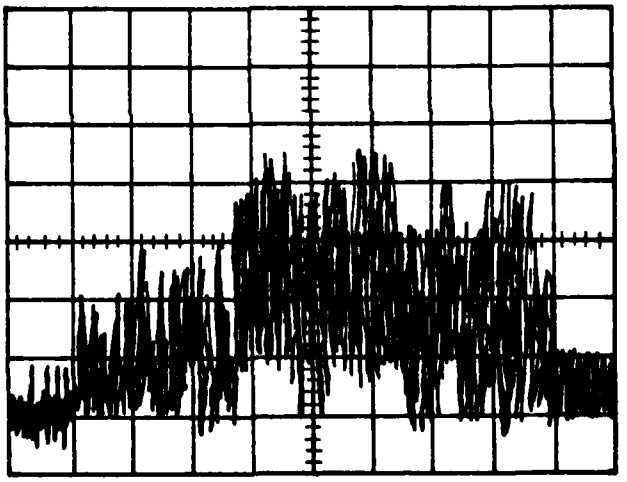

20 MICROSECONDS PER DIVISION

Figure 6.2 Oscillograms from the Video Monitor Oscilloscope Showing Dense Pulse-bursts Associated with Nearby Lightning Flashes.

these cases the impulses ocurred at such a fast rate (in the order of a half-million per second) that the tails of the video pulses overlapped, causing a displacement of the 'zero baseline' for times in the order of 200 microseconds. Similar dense bursts were sometimes seen from storms too far away for lightning flashes to be observed visually. Figure 6.3 gives two examples of pulse-bursts from storm S1, which were recorded on magnetic tape, and displayed on the X/Y plotter. The dense bursts received at Prospect Hill are evidently similar to those described by Harvey (1972). The Megapulse experience supports the idea that dense bursts indicate actual lightning, while impulses ocurring at low rates indicate the presence of less energetic discharges in the clouds. However, an evaluation of the use of the low-rate impulses as an indicator of potential lightning hazards was far beyond the scope of this effort.

The use of radar pictures to supplement the directional display was an essential element in determining source-strength. In the future it would be even more helpful if expanded scale pictures, with a maximum range of perhaps 100 km, could be made available.

The Prospect Hill receiving site is in an urban environment and is surrounded by industrial activity, which results in a level of UHF noise which is undesireably high for the measurement of some impulses. This is especially true when the antenna beam is directed at low elevation angles. Thus, attempts to observe

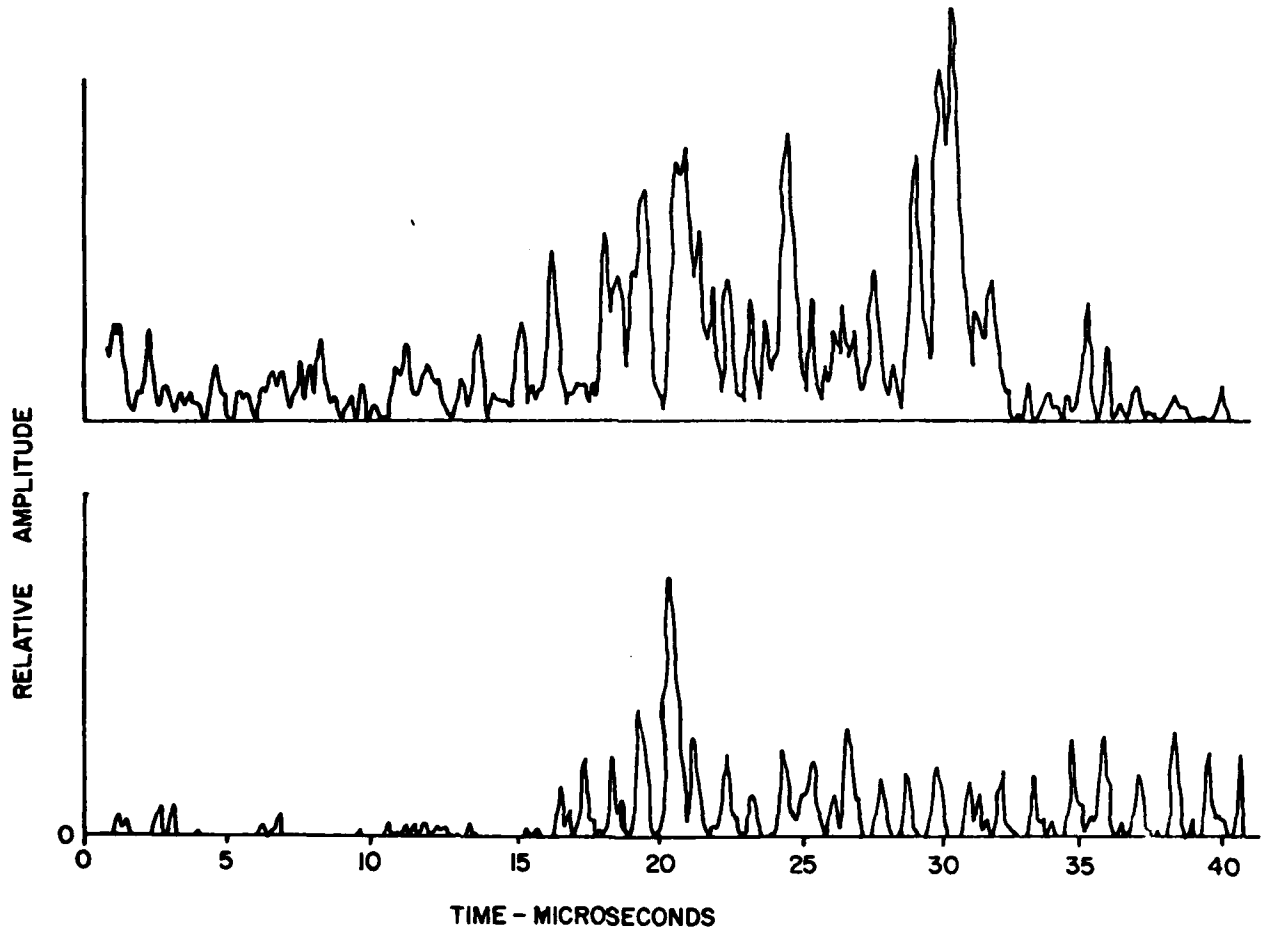

Figure 6.3 Two Examples of Dense Pulse-Bursts from Storm S1.

coronal impulse noise from distant jet aircraft remained inconclusive. Occasionally, impulses were detected from small propeller-driven aircraft passing near Prospect Hill, but it is believed that these impulses came from the engine ignition circuits, rather than corona discharge.

SECTION 7

CONCLUSIONS

The equipment developed under this contract performed as expected, and its use was demonstrated by obtaining new and original spectral source-strength data at 910 MHz. By changing the RF front end, the equipment would be capable of providing similar data at still higher frequencies. The detectability of UHF corona impulses from jet aircraft and missiles remains inconclusive, and will require further study.

REFERENCES

Harvey, R.B. and Lewis, E.A.; "Radio Mapping of 250 to 925 MHz Noise Sources in Clouds", AFCRL-72-0078; 1972.

Harvey, R.B.; "Personal Communication"; 1979.

Horner, F.; "Radio Noise from Thunderstorms", Advances in Radio Research, Saxton, J.A. - Editor, Volume 2, Academic Press; 1964.

Kachurin, L.G., Karmov, M.I., and Medaliyev, Kh. Kh., "The Principal Characteristics of the Radio Emission of Convective Clouds", Izv., Atmospheric and Oceanic Physics, Volume 10, Number 11, pp. 1163 - 1169; 1974.

Lewis, E.A.; "Personal Communication"; 1979.

Lewis, E.A.; "Personal Communication"; 1980.

Lewis, E.A.; "Personal Communication"; 1981.

Nanevicz, J.E. and Hilbers, G.R.; "Flight Test Evaluation of an Active Discharger System", Stanford Research Institute, Menlo Park, California, Interim Report 1; February 1970.

Strom, J.A. and Ehrenspeck, H.W.; "An SBF Array for Reception of Atmospheric Noise", AFCRL-TR-74-0372; 1974.

APPENDIX A

SPECTRAL DENSITY OF THE CALIBRATION PULSE

The pulse generator (Singer Model 91263-1) contained a short length L of a 50 ohm transmission line (see Figure A.1). End A of the section was effectively open circuit, although it was permanently connected through a very high resistance R to a DC voltage V which was step-wise selectable by a decibel attenuator on the instrument panel. End B of the line section was connectable via mercury-wetted relay contacts to the 50 ohm cable running to the receiving equipment. This cable was temporarily disconnected from the receiving antenna in order to inject the calibration pulse.

When the switch is closed, the voltage at the end of the cable jumps from 0 to V/2, and a wave of voltage V/2 starts down the cable toward the receiver. Simultaneously, a wave of voltage -V/2 moves along the line section reaching end A after a time L/v, where v is the velocity of waves on the line. At this time the line section has a uniform voltage of V/2. Upon reflection at end A, the -V/2 wave reverses direction, and after a time L/v reaches the matched end B of the line. At this moment the line section is discharged, and except for slowly recharging through the large resistor R, it remains uncharged. The -V/2 wave continues without reflection into the cable where it cancels the V/2 wave already in progress. The total duration of the V/2 wave in the cable is therefore T = 2L/v, and its time history F(t) is as illustrated in Figure A.2. The manufacturer of the instrument states that $T \simeq 5 \times 10^{-10}$ seconds.

There are different ways of specifying the spectral content of a pulse, depending on how arbitrary multiplying and dividing factors are assigned to the right-hand sides of Equations (2.1) and (2.3). Such factors are typically $\sqrt{2}$ or $\sqrt{\pi}$ or some combination. To be consistent with the convention adopted here and expressed in Equation (2.3), the amplitude spectral density of the calibration pulse is

$$2\int_{-\infty}^{+\infty} F(t)e^{i\omega t}\,dt = 2\int_{0}^{T} \frac{V}{2} e^{i\omega t}\,dt$$

$$\simeq 2\int_{0}^{T} \frac{V}{2}\,dt$$

$$\simeq TV \text{ volts Hertz}^{-1}$$

where, in the last two steps, it is assumed that $\omega T << 1$.

With the voltage selector on the instrument panel in the 40 dB position, the DC voltage on the line was measured at 0.5179 volts. In the 0 dB selector position the voltage $V = 0.5179 \times 10^{-2}$, and taking $T \approx 5 \times 10^{-10}$ sec, the amplitude spectral density $TV \simeq 2.588 \times 10^{-12} \simeq \sqrt{2\pi}\ 10^{-12}$ volts Hertz^{-1}. The manufacturer states that the amplitude spectral density with the selector at 0 dB is 1 μv/MHz or 10^{-12} volt Hertz^{-1} but the convention used is not specified explicitly. It must, therefore, be concluded that the instrument values are to be multiplied by $\sqrt{2\pi}$ to make them consistent with Equation (2.3).

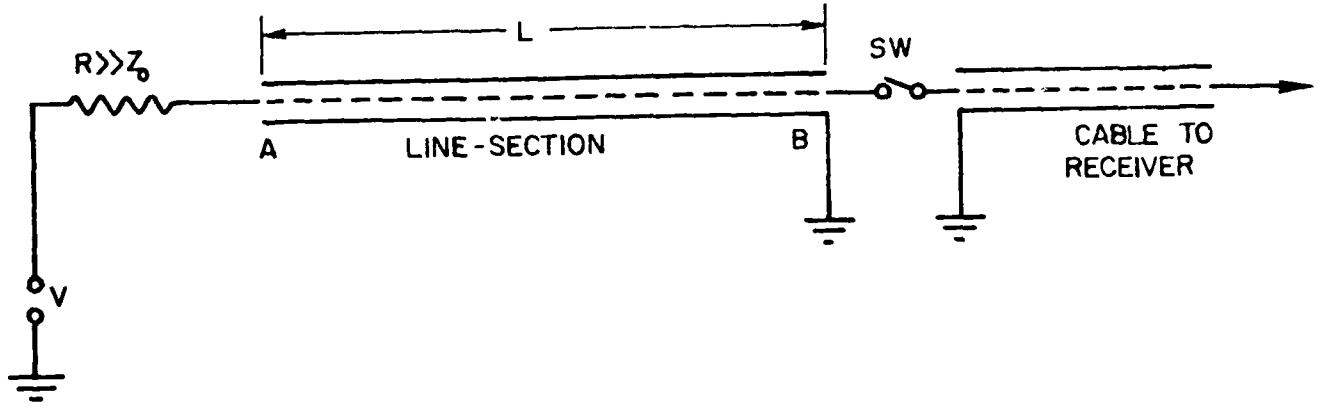

Figure A.1 Essential Elements of Calibration Pulse Generator.

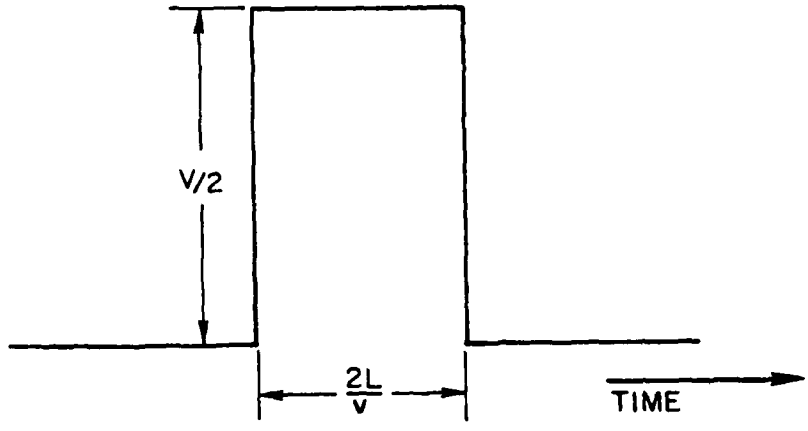

Figure A.2 Illustration of Voltage Impulse.

APPENDIX B

CALIBRATION PROCEDURE

BY

DONALD E. MEYERS, MEGAPULSE, INC.

The calibration (see Figure B.1) of the system was performed by using the Impulse Generator as a known source of signal, and accounting for every gain or loss. Every portion of the system had a large dynamic range. Also, everything was linear over a large range except the receiver; therefore, a linear portion of the receiver was selected and the gain set and locked. Consequently, compatible settings had been set for the waveform recorder to signal averager and the oscilloscope.

The Impulse Generator and the attenuators are set with calibrated switches. During the receiving of an unknown signal, only Attenuator 2 ordinarily would be varied. Therefore, the amplitude of the signal on the oscilloscope and the setting of Attenuator 2 would be directly related to a signal from the Impulse Generator and its amplitude on the oscilloscope. If other items were changed, a new calibration would have to be performed.

The details of the system's calibration follow:

1. Aim the receiver antenna at the monopole.

   Azimuth = 160°; Elevation = 10°

2. Set the Impulse Generator (90 dB).

3. Set AT2 (to zero).

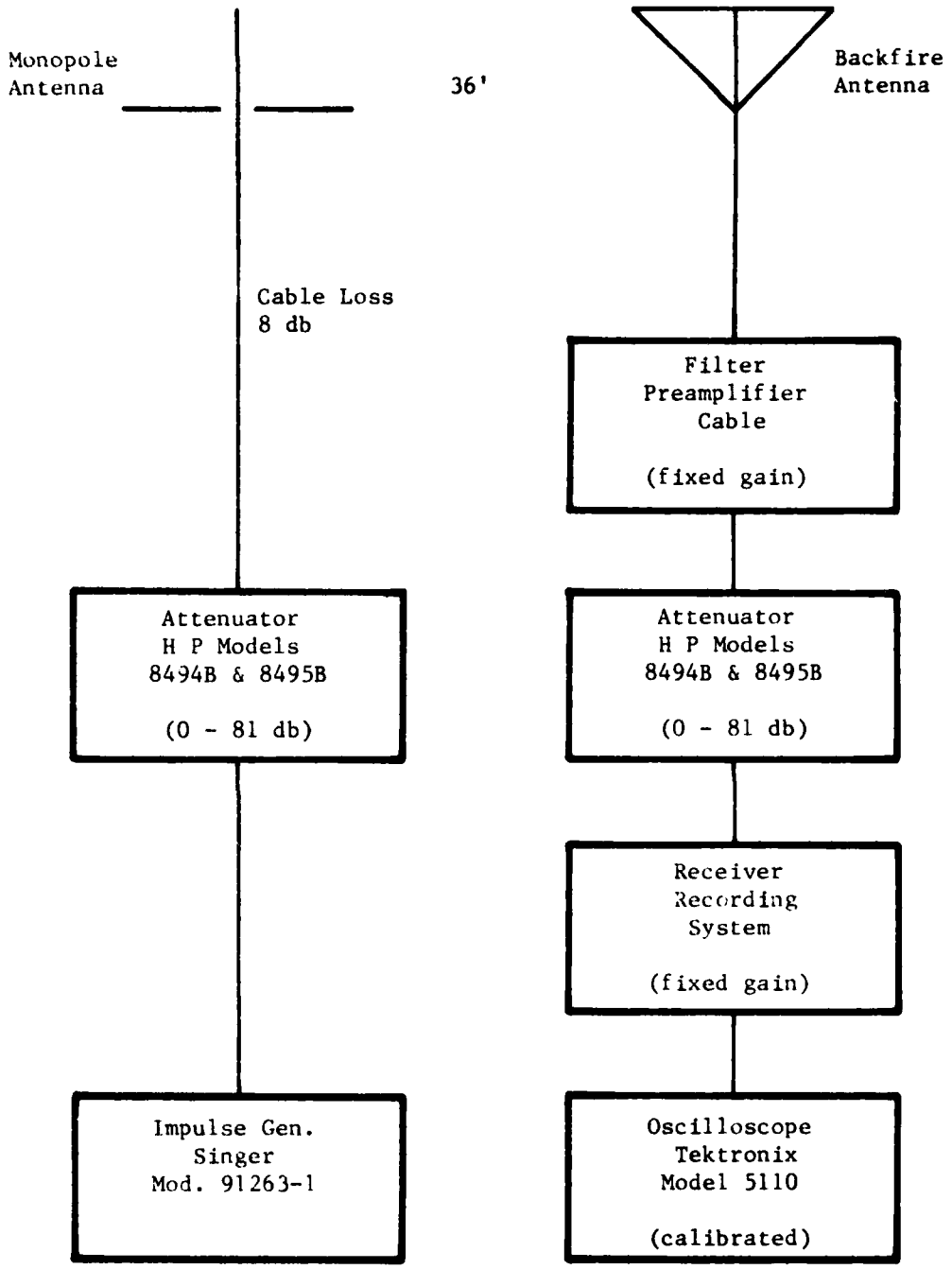

Figure B.1 Block Diagram Calibration System.

4. Adjust AT1 until the signal is at a reference (full scale 8 divisions) on the scope. (A slight adjustment of the receiver might also be necessary.)

5. Record AT1 setting (18 dB).

6. Calculate E_c

$$E_c = 377 \frac{h_e}{\lambda} \frac{1}{D} I_a \text{ mv/meter}$$

E_c = field strength at aperture of receiver antenna in mv/m-mHz

λ = wavelength in cm. = 33.1 cm.

$h_e = \frac{\lambda}{2\pi} \tan \frac{\pi h}{\lambda}$

h = height of the monopole antenna in cm. = 7.62

h_e = 4.54 cm.

D = distance from the calibration antenna to receiver in kilometers = $\frac{9.45m}{1000}$

$I_a = \frac{E_r}{R_a} = 20 \log E_r + 20 \log \frac{1}{R_a}$

R_a = resistance of monopole = 36Ω

E_r = voltage at base of calibration monopole in db re:v/mHz

E_r = Eg - AT1 - Cable loss - 120

E_g = voltage output in db of Impulse generator above 1 uv/mHz = 90 db

AT1 = attenuator setting in db

Cable Loss = 8 db

E_r = 90 - AT1 - 8 - 120

E_r = - AT1 - 38 db

I_a = - AT1 - 38 db - 31.1 = AT1 - 69.1 db

$E_{cdb} = 20 \log 377 + 20 \log \frac{h_e}{\lambda} + 20 \log \frac{1}{D} + 20 \log I_a$

$= 51.5 - 17.3 - 19.5 + 60 + (-AT1 - 69.1)$

E_{cdb} = 5.6 - AT1 For Eg set to 90 db

For Eg Variable

E_{cdb} = Eg - 84.4 - AT

Sample calculation where E_g = 90db and AT1 = 18 db

E_{cdb} = 90 - 84.4 - 18 = -12.4 db re: mv/m-mHz

Therefore an unknown signal (E_s) can be determined by the setting of AT_2 and the pulse height on the oscilloscope. For example, assume that AT_2 was set to 12 and there was a pulse height of 3 divisions:

$$E_s = E_c + AT_2 + 20 \log \frac{\text{Pulse height}}{8}$$

E_s = -12.4 db + 12 db + 12-8.5

E_s = -8.9 db re: 1mv/m-mHz

Table B.1 illustrates the calculation involved in the case of five noise pulses.

Table B.1 Pulse Heights for Thunderstorm on 4 August 1980

Pulse No.	Time GMT.	Distance nm	Amp-litude	Amplitude db ref. 6.8	E_s for E_c = -7.4	Distance db	E_s db re 1MV/m - mhz	En* Vm^{-1} Hz^{-1}
1	2230	16.5	5.1	-2.5	- 9.9	89.7	79.8	1.0×10^{-9}
2	2231	16.5	6.9	0.13	- 7.3	89.7	82.4	1.3
3	2232	16.5	5.8	-1.3	-8.7	89.7	81.0	1.1
4	2234	16.5	4.0	-4.6	-12.0	89.7	77.7	.8
5	2235	16.5	3.4	-6	-13.4	89.7	76.3	.7

*The numbers in this column are to be multiplied by $\sqrt{2\pi}$ for consistency with Equation (2.3), see discussion in Appendix A.

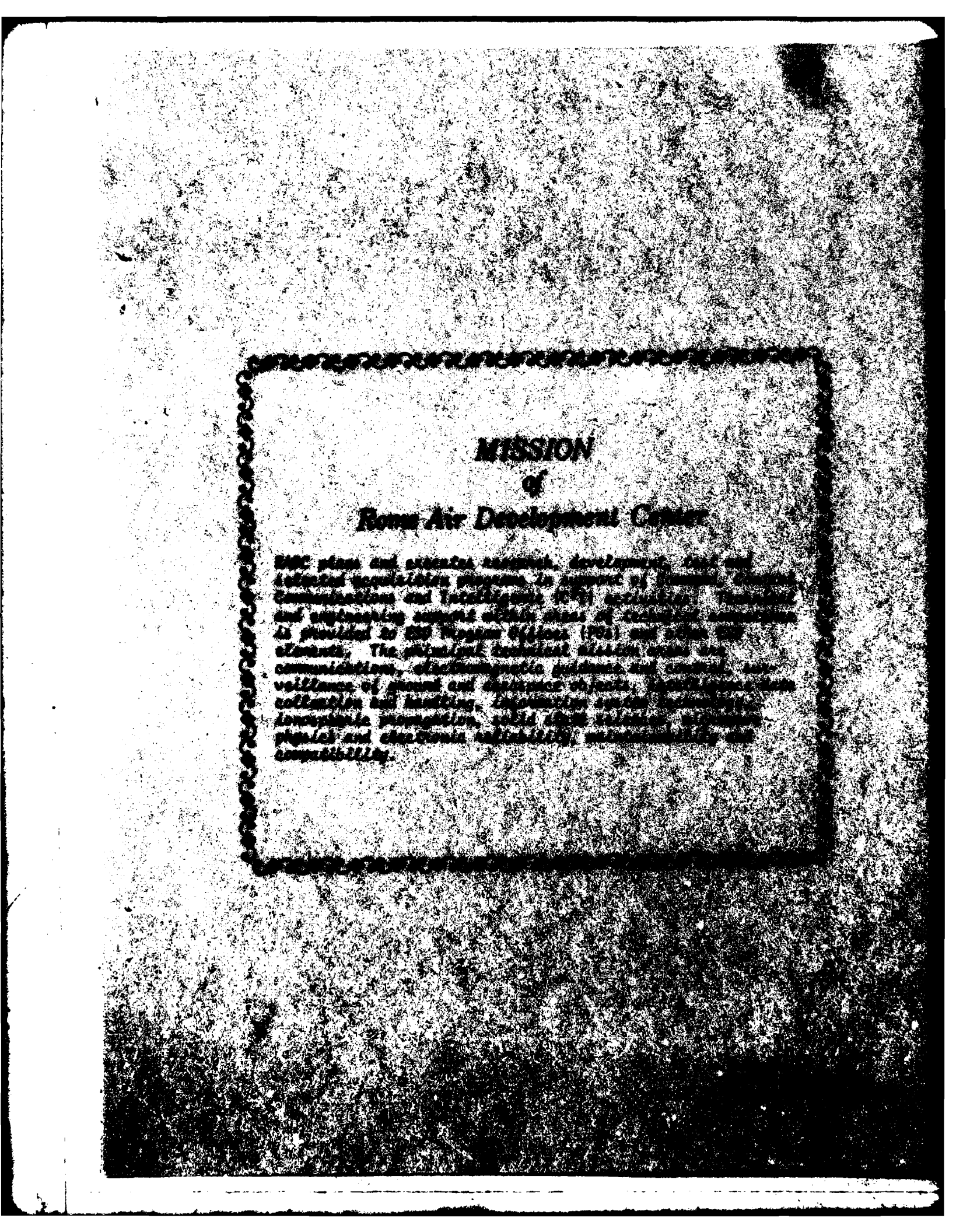
MISSION
of
Rome Air Development Center